Investigation of Impact Angle Effect on Brain Strain Distribution in Football Headers Using a Detailed FE Brain Model

Shingo Kitamura, Yusuke Miyazaki, Jon Farmer, Rory England, Ieuan Phillips

I. INTRODUCTION

Heading the ball is a fundamental movement frequently performed in association football that exposes players to repetitive non-concussive impacts. Repetition of these low-intensity head impacts is believed to contribute to the presentation of long-term degenerative brain diseases, such as chronic traumatic encephalopathy (CTE), later in life. CTE presents with diverse clinical symptoms, including memory loss, depression and motor dysfunction, which are hypothesised to originate from localised neurological damage in specific functional brain regions [1]. Therefore, it is important to understand the distribution of mechanical responses during headers. Since impact angles influence head rotational kinematics and the relative displacement of brain against intracranial structures, analysing strain distribution for different impact angles using a Finite Element (FE) head model is important. However, many of the FE models used in conventional studies simplify complex brain geometries. As complex brain geometries, such as sulci, alter the local distribution of brain strain [2], it is difficult to analyse detail strain distribution using the simplified model. To address this limitation, we constructed a detailed FE head model that reconstructs the complex geometry of the brain. Using this model, we conducted ball-to-head impact simulations at multiple impact angles to analyse detail strain distributions and to consider the effects on brain function.

II. METHODS

Construction of a Detailed FE Head Model

We developed a detailed FE head model, reconstructing cerebral sulci, by integrating an MRI-based brain model with the Total Human Model for Safety (THUMS) AM50 Occupant Model Version 6.1 [3]. The MRI-based brain model was morphed to align with the outer dimensions of the original THUMS brain. Subsequently, a cerebrospinal fluid (CSF) layer was generated between complex brain surface and the inner surface of the THUMS skull. The original brain and CSF parts in THUMS were replaced with these newly developed models. A tied contact was defined between the skull and the CSF to ensure mechanical continuity. The detailed brain and CSF models were meshed using tetrahedral elements, resulting in a total of 2,258,483 elements for the entire head model. The mesh quality was evaluated, confirming that both the Jacobian and aspect ratio were acceptable. The brain and CSF were modelled as a Maxwell viscoelastic material. The material properties for both components were set to the same values as THUMS. The response of the constructed head model was validated against post-mortem human subject (PMHS) experimental data. We simulated frontal impacts [4] to evaluate intracranial pressure (ICP), and rotational impacts [5] to evaluate brain-skull relative displacement. The correlation between the simulation results and the PMHS data was evaluated using the CORA (CORrelation and Analysis) method. The average CORA scores were 0.709 for ICP and 0.559 for relative displacement, which were higher than those of an original THUMS head model (ICP: 0.564, relative displacement: 0.404) [3], confirming the validity of the model.

Ball-to-Head Impact Simulations with Multiple Impact Angles

Using the detailed FE head model integrated with the full-body THUMS, we conducted ball-to-head impact simulations at multiple impact angles (Fig. 1). This model replicates neck muscle activation with PID control. An experimentally validated three-layer ball model of the Adidas Uniforia (air bladder, foam, TPU) with non-linear material properties was utilised. In the ball-to-head impact simulations, the impact angle was defined as the angle between the mid-sagittal plane of the head and the velocity vector of the ball. Simulations were performed at three angles: 0°, 30°, and 60° (Fig. 2). To simulate a typical head impact location, the centre of gravity of the ball was horizontally aligned 10 mm below the vertex. The impact velocity was set to 17 m/s, representing a typical corner kick [6]. The ball inflation pressure was 1.0 bar, close to the upper limit of the manufacturer inflation guidance. The simulation duration was set to 80 ms post-impact, allowing sufficient time for the head angular

S. Kitamura is a MSc student and Y. Miyazaki is an Associate Professor in the Department of Systems and Control Engineering, Institute of Science Tokyo. J. Farmer, R. England and I. Phillips are in the Sports Technology Institute, Loughborough University, UK.

velocity to stabilise. To evaluate the global response of the brain, the peak 95th percentile maximum principal strain (95MPS) was calculated. Also, to investigate the regional strain distribution, the temporal maximum of the maximum principal strain (ε_{max}) was extracted for each element to generate spatial strain distribution maps.

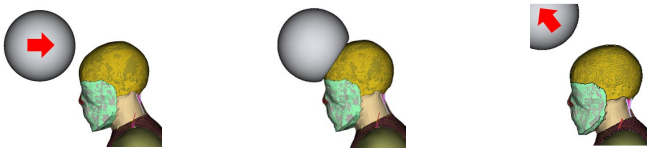

Fig. 1. Sequence of the impact simulation (0°).

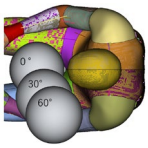

Fig. 2. Impact conditions.

III. INITIAL FINDINGS

The peak 95MPS values were 0.080, 0.114, and 0.146 for the 0°, 30°, and 60° impact angles, respectively. The global brain strain increased as the impact angle increased. The strain distribution patterns for the 30° and 60° oblique impacts were largely similar. The spatial distribution maps of the εmax for the 0° and 60° impacts are shown in Fig. 3. Across all impact conditions, localised high strain was consistently observed in the brainstem. In the 30° and 60° impacts, increased strain compared to the surrounding regions was observed in the temporal lobe, cerebellum, dorsomedial frontal lobe, and occipital lobe. Also, especially large strain was observed in sulci.

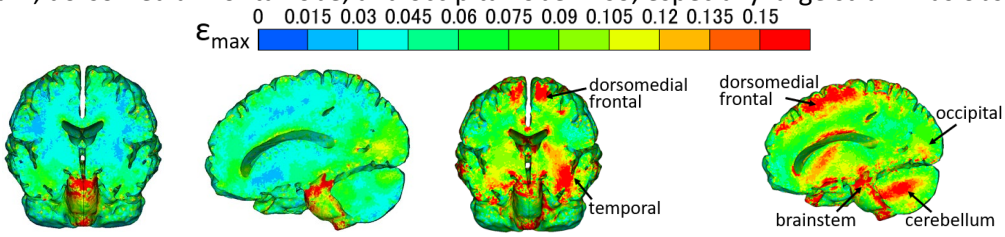

(a) ε_{max} at 0° impact (b) ε_{max} 60° impact

Fig. 3. Distribution of ε_{max}.

IV. DISCUSSION

The peak 95MPS was less than 0.15 in all conditions. If the peak 95MPS can be considered a good indicator for concussion risk, our results indicate that a single header is at a level lower than that reported for concussion occurrence in sports such as American football [7]. Frontal headers demonstrated lower strain magnitudes than those with oblique impact angles. The brain lateral displacement is constrained by the falx cerebri, which separates the left and right hemispheres, resulting in increased strain. These results indicate that different types of header could contribute towards different long-term brain strain exposure. By using the detailed FE head model, we analysed the strain distribution trends in detail. Strain consistently concentrated in the brainstem across all conditions. As the structural junction between the cerebrum and cerebellum, the brainstem is highly susceptible to displacement induced by rotational head kinematics. The increased strain in the temporal lobe during oblique impacts is attributed to complex local anatomies, such as the lateral sulcus. Strains in the cerebellum, occipital lobe, and dorsomedial frontal lobe are likely caused by constraints by the falx cerebri and tentorium cerebelli. The regional strains observed in the brainstem, temporal lobe, cerebellum, and occipital lobe are concurrent with regions that typically present as susceptible to long-term CTE pathologies, including tau lesions and white matter degeneration [8-9]. This indicates that brain strains induced by header could have long-term cumulative effects on brain function. In contrast, while increased strain was observed in the dorsomedial frontal lobe, clinical CTE lesions are predominantly found in the dorsolateral regions [8]. This indicates the necessity for considering a broader range of kinematic factors, such as head rotational kinematics. This study provides a biomechanical basis for safer heading guidelines and future studies will explore various impact locations to evaluate the influence of rotational kinematics on brain strain.

V. REFERENCES

[1] Mez, J., *et al.*, JAMA, 2017.
[2] Johnson, H., *et al.*, *J Biomech*, 2009.
[3] Toyota Motor Corp., *et al.*, Documentation, 2021.
[4] Nahum, A. M., *et al.*, Stapp Car Crash Conf, 1977.
[5] Hardy, W. N., *et al.*, *Stapp Car Crash J*, 2001.
[6] Ferdousi, J., *et al.*, *Sci Rep*, 2023.
[7] Cecchi, N. J., *et al.*, *Ann Biomed Eng*, 2022.
[8] McKee, A. C., *et al.*, *Brain*, 2013.
[9] Koerte, I. K., *et al.*, JAMA, 2012.